# How do pre-existing normal faults influence rift geometry? A comparison of adjacent basins with contrasting underlying structure on the Lofoten Margin, Norway

Gijs Allard Henstra*, Thomas Berg Kristensen, Atle Rotevatn, Rob Gawthorpe

*Department of Earth Science, University of Bergen, PO Box 7800, 5020 Bergen, Norway*

**) corresponding author (gijshenstra@gmail.com)*

**Abstract**

Recent studies of natural, multiphase rifts suggest that the presence of pre-existing faults may strongly influence fault growth during later rift phases. These findings compare well with predictions from recent scaled analogue experiments that simulate multiphase, non-coaxial extension. However, in natural rifts we only get to see the final result of multiphase rifting. We therefore do not get the chance to compare the effects of the same rift phase with and without pre-existing structural heterogeneity, as we may in the controlled environment of a laboratory experiment. Here we present a case study from the Lofoten that provides a unique opportunity to compare normal fault growth with and without pre-existing structural heterogeneity. Using seismic reflection and wellbore data, we demonstrate that the Ribban Basin formed during Late Jurassic to Early Cretaceous rifting. We also show that the rift fault network of the Ribban Basin lacks a pre-existing (Permian-Triassic) structural grain that underlies the neighbouring North Træna Basin that also formed during the Late Jurassic to Early Cretaceous. Being able to compare adjacent basins with similar histories but contrasting underlying structure allows us to identify key characteristics of faults that grow. We demonstrate that in Lofoten, the absence of pre-existing normal faults produced collinear fault zones. Conversely, where pre-existing faults are present, normal fault zones develop strong 'zigzag'plan-view geometries.

## 1. Introduction

The initiation stage of continental rifting is characterised by the nucleation of numerous fault segments. As extension progresses, faults will link to form longer, larger-throw, amalgamated faults (Prosser, 1993; Cowie, 1998; Gupta *et al*., 1998). Continued extension ultimately leads to the localization of the majority of strain onto a smaller number of large, through-going normal faults that bound large (half-) graben basins (Cowie *et al*., 2000; McLeod, 2000; Bell *et al*., 2014). Faults may subsequently link up at deeper crustal levels as a rift progresses from the initial stretching stage to the thinning- and hyperextension stages (Peron-Pinvidic et al., 2013).

Numerous rift basins across the world have formed in response to not one but several distinct phases of extension (*e.g.* the Gulf of Aden, Bellahsen *et al*., 2006; the northern North Atlantic, Nøttvedt *et al*., 2008 and the East African Rift, Macgregor, 2015; the East Greenland rift system, Rotevatn *et al*., 2018a). Such basins are referred to as multiphase rifts if the different rift phases are separated by protracted periods of relative tectonic quiescence (i.e. inter-rift periods that last >10 Myr *cf*. Ravnås *et al*., 2000).

The presence of pre-existing structural heterogeneity in the form of older, buried rift faults may influence the development of normal faults during renewed extension. The propensity of normal faults to be reactivated between subsequent rift phases depends on factors such as the extent of diagenetic fault healing (Tenthorey *et al*., 2006; Laubach *et al*., 2014), the thermal and rheological state of the lithosphere (Bell et al., 2014), and geometrical aspects such as strike and dip (e.g. Etheridge, 1986; Morley, 2016). Deng *et al*. (2017) discuss styles of normal fault reactivation during multiphase rifting and distinguish between upward propagation and vertical linkage (see also Walsh *et al*., 2002; Giba *et al*., 2012). Claringbould *et al*. (2017), however, demonstrated that not all multiphase-

rifted basins involve reactivation of pre-existing normal faults (see also Lee and Hwang, 1993; Tomasso et al., 2008). In cases where pre-existing structural fabric (faults or shear zones) is not reactivated directly, the presence of crustal heterogeneity may still exert control by influencing the location and reorienting the strike of younger rift faults (Phillips *et al*., 2016; Rotevatn *et al*., 2018a)

During multiphase rifting, the direction of extension may or may not vary between successive rift phases (e.g. Davies *et al*., 2001; Morley *et al*., 2004; Morley, 2016). Scaled analogue experiments that simulate two phases of non-coaxial extension indicate that the presence of pre-existing normal faults can strongly influence fault growth during renewed, but differently-directed, extension (Keep & McClay, 1997, Henza *et al*, 2011). Natural examples of major normal faults that formed over several distinct phases of extension with varying extension directions (i.e. non-coaxial multiphase extension) typically form amalgamated structures comprised of fault segments with various angles (*e.g*. Whipp *et al*., 2014; Henstra *et al*., 2015). These case studies suggest that certain observations from scaled analogue experiments also apply to natural rifts: reactivation tends to be selective and oblique, whereas new faults may strike obliquely to orthogonally to second-phase extension under the influence of first phase structures. This leads to the development of zigzag- and crosscutting geometries (cf. Henstra *et al*., 2015). However, these case studies of natural rifts document the end-result of multiphase rifting. Contrary to the controlled environment of the scaled analogue experiments, this means that we cannot know with absolute certainty which lithospheric parameters (e.g. the presence of pre-existing structural heterogeneities) controlled the final plan-view morphology of rift faults. In this paper we explore the role of pre-existing normal faults on the plan-view development of fault arrays that formed by reactivation in nature.

Previous studies of the North Træna Basin (Henstra *et al*., 2015) and the Vestfjorden Basin (Fig. 1; Doré *et al*., 1999; Wilson *et al*., 2006; Bergh *et al*., 2007; Hansen *et al*., 2012) are compared to new analysis of 2D seismic reflection data from the Ribban Basin (Fig. 1). This allows us to compare the plan-view geometry and structural history of the Lofoten Margin's four major fault zones. It was shown before that the East Røst Fault Zone and the Vesterdjupet Fault Zone are Late Jurassic–Early Cretaceous faults with a strong Permian–Triassic ancestry (Henstra *et al*., 2015). Here we demonstrate that the West Lofoten Boundary Fault Zone that bounds the Ribban Basin is a Late Jurassic–Early Cretaceous fault that formed over an area where the pre-existing Permian–Triassic structural grain was absent, or at least significantly less developed. The same applies to the East Lofoten Boundary Fault Zone that bounds the Vestfjorden Basin. The uniqueness of this setting, with adjacent basins with contrasting underlying structure, allows for a comparative study of fault growth in i) a basin where the imprint of initial phase extensional faulting is strong (North Træna Basin), versus ii) a basin where this imprint is weak (Ribban Basin). As such, the Lofoten Margin is ideal for an investigation into the impact of having, or not having, a pre-existing network of rift faults during renewed rifting.

## 2. Tectonic history of the multiphase rifted Lofoten Margin

The Lofoten Margin is located on the northernmost segment of the Norwegian Passive Continental Margin (Fig. 1a). It forms an integral part of the northern North Atlantic conjugate margins of Norway and Greenland. The Norwegian Passive Continental Margin developed in response to a protracted period of episodic rifting between Greenland and Norway that lasted throughout the late Palaeozoic and Mesozoic until continental break-up gave way to oceanic spreading in Palaeogene times (Doré, 1992; Faleide *et al*., 2010). Palaeozoic-Mesozoic rifting was preceded by Devonian orogenic collapse and unroofing of thickened continental crust that had formed along the suture between Baltica and Laurentia during the Caledonian orogeny (Andersen *et al*., 1991; Klein *et al*., 1999).

In Lofoten, the post-Caledonian exhumation phase lasted into the Permian at which time it was facilitated by the development of a metamorphic core complex (Steltenpohl *et al*., 2004; Henstra & Rotevatn, 2014). The core complex formed in response to a regional top-to-the-east detachment zone (Hames and Andresen, 1996). The exhumed metamorphic core is underlain by a mantle dome (Mjelde & Sellevoll, 1993) and encompasses the central Ribban Basin, the Lofoten Ridge and the southwesternmost islands of the

Lofoten archipelago that consist of granulite and eclogite facies (Steltenpohl et al., 2004, 2006). The development of a core complex in Permian times was followed directly by rifting in the Early Triassic (Hansen *et al*., 1992; Færseth, 2012). This Permian–Triassic rift episode is recognised across the northern North Atlantic rift system (Doré *et al*., 1999; Faleide *et al*., 2010) and was followed by a *c*. 80 Myr long inter-rift period that lasted into the Middle Jurassic (Faleide *et al*., 2010).

The magnitude of Late Jurassic rifting was relatively modest in Lofoten in comparison to the rest of the Norwegian Continental Shelf. The Early Cretaceous, however, represents a major rift episode (Løseth & Tveten, 1996; Tsikalas *et al*., 2001; Hansen *et al*., 2012; Henstra *et al*., 2015). By middle Cretaceous times, three major, sub-parallel extensional basins had developed: the North Træna Basin, the Ribban Basin and the Vestfjorden Basin, separated by two narrow horsts: the Marmæle Spur and the Lofoten Ridge (Fig. 1b). The basins are bounded by four major fault zones that are described here in more detail.

### 2.1 The East Røst Fault Zone (ERFZ)

The ERFZ forms the western margin of the northern part of the North Træna Basin and consists of a single NNE-SSW-striking segment (Fig. 1b). To the south it splits into several NNE-SSW-striking splays (Hansen *et al*., 2012). The northern part of the North Træna Basin was uplifted and partly eroded in Late Cretaceous-Palaeogene times, for which reason the original length of the ERFZ is unknown (Færseth, 2012). The upward termination of the ERFZ falls within the Lower Cretaceous (Fig. 2). The fault continues downward into the acoustic basement and the lower termination is not imaged.

The hanging wall of the ERFZ consists of a Mesozoic interval, the base of which is drilled and assigned an earliest Triassic age (Hansen *et al*., 1992). The underlying interval is interpreted to be of Permian age (Fig. 2; Bergh *et al*., 2007; Hansen *et al*., 2012; Henstra & Rotevatn, 2014). The Permian–Triassic basin-fill consists of syn-rotational strata that exhibit thickening towards the ERFZ (Fig. 2). Thickening towards the ERFZ is also observed for the Lower Cretaceous interval, which is also thicker in the hanging wall to the ERFZ than on its footwall (Henstra *et al*., 2015). Henstra & Rotevatn (2014) argued that the ERFZ initially formed the breakaway fault at the western end of the Permian core complex. The expansion of Triassic strata towards the ERFZ suggests that the fault continued to grow after the core complex became inactive in Early Triassic times. The ERFZ was subsequently reactivated one last time during the Early Cretaceous (Bergh *et al*., 2007; Henstra *et al*., 2015).

### 2.2 The Vesterdjupet Fault Zone (VFZ)

The VFZ is the main border fault to the North Træna Basin, bounding the basin to the east. It consists of two prominent NNE-SSW-striking segments that are linked by a subordinate NE-SW-striking segment (Fig. 1b; Henstra *et al*., 2015). To the north, the VFZ splits up into several NE-SW-striking splays. To the south it links up with the southwestern extension of the Lofoten Ridge. The VFZ has an upward termination in the Upper Cretaceous for most of its length, except for the northernmost NNE-SSW-striking segment that terminates in the Palaeogene (Fig. 2; Henstra *et al*., 2015). The Palaeozoic interval in the hanging wall to the ERFZ is not present in the eastern margin of the North Træna Basin; hence, the acoustic basement in the hanging wall to the VFZ coincides with the seismic marker that represents the drilled Triassic-basement contact (Fig. 2; Hansen *et al*., 1992). The strata that make up the Lower Triassic interval contain occasional growth sequences in association with normal faults, including the two NNE-SSW-striking segments of the VFZ (Henstra *et al*., 2015).

Where drilled, Lower Cretaceous strata of the North Træna Basin rest directly on Middle Jurassic strata. Hansen *et al*. (2012) and Henstra *et al*. (2015) argued that an Upper Jurassic interval is likely present away from the drill site, in the immediate VFZ hanging wall (Fig. 2). This interval is expressed as a series of relatively small (< 15 km long), semi-isolated depocenters that consist of syn-rotational basin-fills (Bergh *et al*., 2007; Hansen *et al*., 2012; Henstra *et al*., 2015). The Upper Jurassic depocentres are interpreted

112 to have formed in response to the development of numerous NE-SW-striking faults along the eastern margin of the North Træna
113 Basin. This second period of extension led to reactivation of the Triassic faults as well as their linkage by a NE-SW-striking segment
114 (Henstra *et al*., 2015).

115 A thick succession of Lower Cretaceous strata is present across the North Træna Basin (Bergh *et al*., 2007; Henstra *et al*., 2015).
116 This interval represents the fill of a full graben, bounded by the ERFZ in the west and the VFZ in the east (Fig. 2). The fact that the
117 Lower Cretaceous interval of the North Træna Basin reflects the development of a single, through-going depocentre as demonstrated
118 by Henstra *et al*. (2015) indicates that the Triassic and Jurassic segments became reactivated again during the Early Cretaceous to
119 form a through-going fault zone.

120 2.3 The West Lofoten Boundary Fault Zone

121 The WLBFZ is characterised by a series of 20-50 km long NE-SW-striking segments that are linked by relatively short NNE-SSW-
122 striking segments (Fig. 1b). The Lower Cretaceous, Upper Cretaceous and Palaeogene intervals resemble basin-wide half-graben
123 basin-fills that thicken into the WLBFZ (Fig. 2; Hansen *et al*., 1992; Bergh *et al*., 2007; Hansen *et al*., 2012; Henstra *et al*., 2017).

124 Shallow drillcores penetrated crystalline basement in the northern Ribban Basin where it is overlain by Middle Jurassic strata
125 (Hansen *et al*., 1992). Seismic studies have shown that the nature of the basement-sediment interface changes southward where the
126 basement is interpreted to be overlain by younger, Cretaceous strata (e.g. Hansen *et al*., 2012). The only reflection that can be traced
127 confidently across the basin is the Base Cretaceous. Interpretations of the pre-Cretaceous basin fill of the southern Ribban Basin
128 vary significantly between studies due to a lack of drilling data. Tsikalas *et al*. (2001) and Hansen *et al*. (2012) tentatively assign a
129 Palaeozoic and/or lower Mesozoic age whereas Doré *et al*. (1999) suggest the oldest sedimentary rocks are of Jurassic age.

130 2.4 The East Lofoten Boundary Fault Zone

131 The seismic dataset that covers the Vestfjorden Basin is much sparser than that of the other basins and no wells have been drilled
132 there. Hence, the structural history of the ELBFZ cannot be resolved with as much confidence as for the other fault zones at present.
133 The lowermost seismic reflection that has been assigned a reasonably confident age is the Base Cretaceous (Hansen *et al*., 2012).
134 Pre-Cretaceous strata in the immediate foot- and hanging wall of the ELBFZ that may be of either Palaeozoic or lower Mesozoic
135 age exhibit westerly onlap and lack a syn-rotational geometry (e.g. Fig. 1c; Doré *et al*., 1999; Hansen *et al*., 2012).

136 In the northern part of the Vestfjorden Basin, away from the ELBFZ, a NNE-SSW-trending fault-bounded depocentre with pre-
137 Cretaceous fill is observed (Bergh *et al*., 2007). These fault zones have a similar trend as the NNE-SSW-striking Permian brittle
138 structural grain observed onshore on the Lofoten islands (Klein *et al*., 1999; Steltenpohl *et al*., 2004). The Lower Cretaceous interval
139 is interpreted as the infill of a wide depocentre that formed in response to Early Cretaceous activity of the ELBFZ (Fig. 1c; Bergh
140 *et al*., 2007).

141 **3. Data and methods**

142 We make use of 2D seismic reflection data that covers the Ribban Basin (Fig. 3). Line spacing is variable but shown in Figure 3.
143 Seismic resolution of the interval of interest varies from 25 to 40 Hz. With an interval velocity of 3000 m/s for sedimentary rocks
144 between 1 and 2.5 s TWTT this yields the vertical resolution: c. 40–60 m. Three key stratigraphic surfaces are identified in shallow
145 wells drilled in the northernmost part of the Ribban Basin and in the North Træna Basin: Basement, Base Jurassic and Base
146 Cretaceous ((Fig. 3; Hansen *et al*., 1992). These surfaces are correlated to their seismic expression by the generation of synthetic

seismograms (Hansen *et al*., 1992). These seismic horizons, in addition to the Base Upper Cretaceous and Top Upper Cretaceous, are furthermore tied to the North Træna Basin that we mapped previously (Henstra *et al*., 2015).

Some structures mapped on seismic are converted from the time- to the depth domain in order to be able to calculate dip angles described throughout this paper. For the sedimentary succession we apply a velocity model that is generated using stacking velocities (Henstra *et al*., 2015). Reflections within the crystalline basement are converted using an interval velocity of 6000 m/s (following Mjelde & Sellevoll, 1993).

## 4. Seismic mapping within the Ribban Basin

In this section we present the results of mapping the Ribban Basin using 2D seismic reflection data. The stratigraphic make-up of the hanging wall depocentres changes from north to south, for which reason we distinguish a northern, a central and a southern area (Fig. 4).

### 4.1 Northern area

Shallow core 6814/04-U-01 drilled through Upper Jurassic and Middle Jurassic strata directly overlying weathered gneiss (Fig. 3; Hansen *et al*., 1992). The Basement surface has a clear expression on seismic data (line 4, Fig. 5). The Jurassic can be mapped with high confidence in the northernmost part of the Ribban Basin (Fig. 4). The basement contact is offset by a number of NE-SW- to NNE-SSW-striking faults that terminate within the Upper Jurassic (line 4, Fig. 5). The Jurassic unit itself exhibits a wedge-shaped basin-fill geometry adjacent to the northern segment of the WLBFZ. A part of the wedge is folded (line 4, Fig. 5).

The Base Cretaceous horizon was sampled by shallow core 6814/04-U-02 (Fig. 3; Hansen *et al*., 1992). This horizon can be mapped across the northern area and is offset only by the WLBFZ. Lowermost Cretaceous strata onlap the folded Jurassic wedge (line 4, Fig. 5). This indicates that the fold formed sometime at the transition from the Late Jurassic to the Early Cretaceous. It is located immediately north of a NNE-SSW-striking splay fault that branches off from the main WLBFZ (line 4, Fig. 4). Such hanging wall folds over ramp flat-structures are commonly interpreted to represent roll-over anticlines that form in response to fault linkage (e.g. Ehrlich and Gabrielsen, 2004; Rotevatn and Jackson, 2014). We therefore interpret the fold of line 4 to be associated with strain localisation on the easternmost fault of line 4 (Fig. 5) during the Early Cretaceous.

Intra-basement reflections seen on line 4 (Fig. 5) are dipping c. 15° due west and most likely represent the deeper expression of the WLBFZ that is imaged rather obliquely by line 4 (Fig. 4).

### 4.2 Central area

The Jurassic unit of the northern area pinches out towards the central area. There, the Lower Cretaceous unit directly overlies basement (line 3, Fig. 5). The basement contact is rather irregular in comparison to the northern area, with regular occurrence of 1-2 km wide, concave features that are c. 100–300 m deep (line 3, Fig. 5). These irregularities may represent heterogeneities in the basement that subcrops the Lower Cretaceous. Alternatively they may represent topographic features on the Base Cretaceous surface such as valleys that formed when the central area was subaerially exposed prior to Cretaceous flooding. The Lower Cretaceous itself represents a broad NE-SW-trending half-graben that thickens into the WLBFZ. The WLBFZ tips out within the Lower Cretaceous.

Intra-basement reflections show a complex network of both east- and west-dipping reflections (line 3, Fig. 5). The west-dipping reflections occur in a narrow band that dips *c*. 20° to the NW and may represent the downward continuation of the WLBFZ similar

to the basement reflections seen in the northern area. The east-dipping reflections form undulating bundles that occur at several levels and are broadly parallel to the basement-sediment surface (lines 3 and 5; Figs. 5 & 6). These reflections are unlikely to be associated with the east-dipping WLBFZ since they appear to be truncated by the west-dipping reflections. The east-dipping basement-parallel reflections are therefore interpreted to represent an older basement fabric.

### 4.3 Southern area

The lowermost horizon that can be linked to the drillcores in the northern area is the Base Cretaceous. This horizon is underlain by a relatively thin unit with a clear syn-rift architecture, consisting of several adjacent half-grabens (Fig. 4; line 2, Fig. 5). The lower boundary of this syn-rift unit is represented by a rather chaotic set of reflections that is interpreted as the basement-sediment interface. Based on similarities in both seismic facies and seismic-stratigraphic architecture, the pre-Cretaceous syn-rift unit of the southern area of the Ribban Basin is correlated to the Jurassic units of the northern Ribban Basin and the North Træna Basin (lines 2 and 4, Fig. 5; Henstra et al., 2015).

The Lower Cretaceous is expressed as a wide, NE-SW-trending graben that thickens into the WLBFZ. Compared to the northern and central areas, the Lower Cretaceous unit is a lot thinner in the southern area (>2000ms and *c.* 500ms TWTT, respectively). The younger basin-fill has been preserved here as well; it indicates that the WLBFZ remained active well into the Palaeogene. The WLBFZ consists of several sub-parallel, NE-SW-striking fault strands that are separated by 2–6 km wide terraces (Fig. 4). The Palaeogene unit is only bounded by the easternmost fault strand (line 2, Fig. 5).

Reflectivity within the basement in the immediate hanging wall of the WLBFZ is less obvious in the southern area (line 2, Fig. 5). Farther up-dip, to the northwest, line 1 (Fig. 2) shows that intra-basement reflections have a pattern that is similar to those of the central area, with east-dipping reflections that are broadly parallel to the basement-sediment interface and west-dipping reflections that may represent the downward continuations of Jurassic–Cretaceous faults.

### 4.4 Structural framework of the WLBFZ

Our analysis of basin-fill architecture of the Ribban Basin reveals that the oldest depocentres associated with the WLBFZ are of Upper Jurassic age. The basin first emerged as two separate NE-SW-trending sub-basins in Late Jurassic times (Upper Jurassic depocentres, Fig. 4). Both sub-basins consist of numerous isolated faults that were incepted during the Late Jurassic. The area in between these two sub-basins, immediately west of Moskenesøy, remained high and was not transgressed until Early Cretaceous times.

Most Jurassic faults of the Ribban Basin are truncated by the Base Cretaceous horizon (Fig. 5). This indicates that dring the Early Cretaceous, most Jurassic faults became inactive as strain became focused on fewer throughgoing faults. In most places the Lower Cretaceous Ribban Basin is bounded by single boundary faults, apart from local areas that most likely resemble breached overlap zones of Jurassic fault segments (Fig. 4). Transverse anticlines developed in the central areas at Early Cretaceous segment boundaries (Figs. 4 & 6). This resulted in the fact that sub-basins remained distinct depocentres throughout the Early Cretaceous even though the northern and southern areas had become linked.

After the Early Cretaceous rift event, the WLBFZ most likely became less active for a period until extension resumed during Late Cretaceous–Palaeogene times (see also Hansen et al., 2012; Færseth, 2012). Because the Upper Cretaceous and younger strata were eroded from the central and northern areas, the stratigraphic response of this younger rift event is only observed in the southern area. The fault strand that bounds the Lower Cretaceous on line 2 (Fig. 5) became abandoned during the early Palaeogene and

displacement was focused on a younger fault farther east. This indicates that strain migrated toward the footwall as rifting progressed.

# 5. Discussion

## 5.1 Tectonic history of the Ribban Basin as part of the multiphase rifted Lofoten Margin

The structural evolution of the Ribban Basin is relatively simple in comparison to that of the North Træna Basin which has a complex Permian-Triassic ancestry (Fig. 7a-b). Given that strata older than Middle Jurassic are interpreted to be absent in the Ribban Basin, we conclude that the WLBFZ is a relatively young structure that was incepted during the Late Jurassic in the central zone of the Permian core complex that had remained an exposed basement high until Middle Jurassic times (Henstra & Rotevatn, 2014). It first became a through-going fault zone towards the end of the Early Cretaceous, when the southern and the northern segments of the WLBFZ linked up (Fig. 7d).

The stratigraphic architecture of the Palaeozoic or lower Mesozoic interval in the foot- and hanging wall of the ELBFZ, with parallel and onlapping geometries, suggests that no fault had formed there prior to the Late Jurassic (Fig. 1c; Doré *et al*., 1999; Hansen *et al*., 2012). The overlying Lower Cretaceous basin-fill on the other hand has a strong wedge-shaped geometry that shows thickening toward the fault (Fig. 1c; Doré *et al*., 1999; Hansen *et al*., 2012). So, although the evolution of the ELBFZ remains poorly constrained due to the sparse dataset and lack of well data, it most likely has a tectonic history that is very similar to that of the WLBFZ, with inception during the Late Jurassic followed by rift climax during the Early Cretaceous (Doré *et al*., 1999).

The main difference between the structural histories of the four main fault zones of the Lofoten Margin is that both the ELBFZ and the WLBFZ nucleated during Jurassic–Cretaceous rifting, whereas the VFZ and ERFZ formed in response to both Permian–Triassic rifting as well as Jurassic–Cretaceous rifting (Fig. 7). These two composite rift phases are henceforth referred to as Phase 1 and Phase 2, respectively.

The two rift phases had a distinct style. The Permian basins that underlie the North Træna Basin, and most likely the Vestfjorden Basin, are mostly east-dipping and formed in the upper plate of a regional top-to-the-east core complex (Fig. 8a-b; Henstra & Rotevatn, 2014). Conversely, the VFZ and WLBFZ are dipping to the west (Fig. 8e). These faults are furthermore shallow-dipping and their lower ends appear to link up in some places (e.g. Fig. 2). This was also noted by Tsikalas *et al*. (2001) and Bergh *et al*. (2007) who suggested that both fault zones sole out into a sub-horizontal detachment zone located in the lower crust. The Permian–Triassic top-to-the-east regime had thus been replaced by a top-to-the-west regime by the Early Cretaceous west of the Lofoten Ridge (Fig. 8).

## 5.2 The distribution of Permian–Triassic faults as a primary control on Jurassic–Cretaceous fault geometry, morphology and basin physiography on the Lofoten Margin

The Lofoten Margin is characterised by a strong contrast in orientation between faults that formed during Phase 1 (predominantly NNE-SSW-oriented; Fig. 9) and those that incepted during Phase 2 (predominantly NE-SW-oriented; Fig. 9). Under the assumption that rift faults preferentially form orthogonally to the regional extension vector (e.g. Keep & McClay, 1997; Acocella *et al*., 2000), the observed difference in strike between Phase 1 and Phase 2 faults fits well with a regional change in extension direction, from broadly E-W in the Permian–Triassic to NW-SE during the Cretaceous, that has been invoked by several authors (e.g. Doré *et al*., 1999; Mosar *et al*., 2002; Wilson *et al*., 2006; Faleide *et al*., 2010).

The WLBFZ and ELBFZ are characterised by a series of 20-50 km long NE-SW-striking Phase 2 segments that are linked by relatively short NNE-SSW-striking segments (Figs. 4 & 7d). We observe no Phase 1 faults or depocentres in the area in which the WLBFZ and the ELBFZ formed. We attribute this to the fact that this area corresponds to the rigid central zone of the Permian core complex (Figs. 8 & 9). We conclude that there was very little or no brittle faulting during Phase 1 in the area that encompasses the Ribban Basin and the Lofoten Ridge (Fig. 7a–b). The absence of Phase 1 faults implies that reactivation played no role in the evolution of the WLBFZ and ELBFZ. Moreover, metamorphic fabrics in the exhumed central zone will be shallowly dipping and may therefore be sub-optimally-orientated for reactivation as (steeper) normal faults. Such intra-basement dip-slope-parallel reflections can be seen in lines 3 and 5 (Figs. 5 & 6) and sections e, h and m of Hansen *et al*. (2012). We conclude that these two fault zones evolved through the growth and linkage of NE-SW-striking fault segments that all incepted during Phase 2. The relatively short NNE-SSW-striking linking segments of the WLBFZ and ELBFZ support existing models for fault growth in response to unidirectional extension of a homogeneous substrate. Models of fault growth describe how, inevitably, zones of overlap (relay zones) will develop between individual fault segments (e.g. Peacock & Sanderson, 1991; Childs *et al*., 1995; Walsh *et al*., 2002; Finch *et al*., 2017). Continued extension may result in fault linkage as a result of displacement accrual and relay rotation/breaching (Jackson & Rotevatn 2013; Rotevatn *et al*., 2018b). Linkage between faults is possible where overlap zones are relatively narrow (Acocella *et al*., 2000). Without a change in the extension vector or an inherited structural grain, this process produces rather straight, or collinear, segmented fault zones as seen both in nature (Crider & Pollard, 1998; Acocella *et al*., 2000) and in laboratory experiments (Keep & McClay, 1997; Henza *et al*., 2011; Rotevatn *et al*., 2018b).

We conclude that there exists a causal relationship between i) the presence or absence of Phase 1 faults and ii) the plan-view geometry of through-going fault zones that emerged during Phase 2 rifting. Where a well-developed set of Phase 1 faults is present, such as in the North Træna Basin (Henstra et al., 2015), we observe the development of Phase 2 fault zones that have an overall NNE-SSW-strike and exhibit strong zigzag geometries. Conversely, where Phase 1 faults are absent, we observe the development of Phase 2 fault zones that are collinear and strike NE-SW. In other words, the differences in plan-view geometry between the VFZ and ERFZ on the one hand and the WLBFZ and ELBFZ on the other are ascribed to variability in the pervasiveness of Phase 1 faults.

### 5.3 Fault growth in multiphase rifts

We have argued that the presence of inherited rift faults exerted a major control on normal fault growth during subsequent rift phases. In Lofoten, this control is manifested in three ways: i) the dominant segments of through-going rift faults that grow by reactivation of a pre-existing rift fabric tend to strike obliquely to the prevailing extension direction (Fig. 10a–d); ii) through-going rift faults that are able to grow by (oblique) reactivation of a pre-existing rift fabric tend to exhibit strong zigzag geometries (Fig. 10a–d) and iii) the development of splay faults in foot- and hanging wall that develop at an angle to the reactivated Phase 1 segments but orthogonal to the direction of Phase 2 extension (Fig. 10c–d). Normal fault zones with splays and zigzag geometries that have a comparable multiphase-rift history have been described by Lepvrier *et al*. (2002) and Whipp *et al*. (2014). Conversely, where no pre-existing rift fabric exists, normal faults tend to evolve as collinear faults that strike orthogonally to the prevailing extension direction during Phase 2 (Fig. 10e–h).

These findings are in good agreement with observations made in scaled analogue experiments that simulate non-coaxial multiphase extension (Keep & McClay, 1997; Henza *et al*., 2011). In these experiments it was observed how the presence of Phase 1 faults resulted in the development of segmented faults with strong zigzag- and cross-cutting plan-view geometries during Phase 2 whereas the absence of Phase 1 faults lead to the development of collinear segmented faults that formed orthogonal to the direction of extension during Phase 2 (Fig. 9). It was furthermore observed by these workers how Phase 2 splay faults typically form at the tips

293 of Phase 1 faults. This phenomenon may explain the origin of zigzag geometry of many segmented normal faults in non-coaxial
294 multiphase rifts (Fig. 9d; Henza *et al*., 2011; Whipp *et al*., 2014)

295 Why do pre-existing faults play a dominant role in some multiphase rifts, like the Lofoten Margin (see also North Sea Rift, see
296 Phillips et al., 2016; East Greenland Rift, e.g. Rotevatn et al., 2018a), but not in others (e.g. Shetland Basin, Claringbould *et al*.,
297 2017)? One factor that may have contributed to the high degree of fault reactivation in Lofoten relates to the geometry/orientation
298 of Phase 1 faults: those Phase 1 faults that became reactivated were relatively steeply dipping (Fig. 2) and had a strike less than 45°
299 from perpendicular to NE-SW-directed extension during Phase 2 (Fig. 8). These are geometrical aspects that may significantly
300 improve the likelihood of reactivation (Etheridge, 1986; Huyghe & Mugnier, 1992; Henza et al 2010; Deng et al., 2017).

301 Another clue that may explain why Phase 1 faults of the Lofoten Margin had a strong propensity for reactivation is the fact that they
302 juxtapose rocks with very different properties: siliciclastic rocks in the hanging wall against lower crustal crystalline basement in
303 the footwall. The heterogeneity produced by these Phase 1 faults was likely to be subject to substantial stress concentration from
304 the outset of Phase 2. We speculate that these faults were therefore likely subjects for strain localisation leading to their reactivation,
305 since the juxtaposition of lithologies of contrasting mechanical properties is perhaps more likely to preserve the fault as a significant
306 mechanical discontinuity even in if the fault itself heals. This hypothesis may also help explain why pre-existing faults that juxtapose
307 similar lithologies on either side of the fault in some other multiphase rifts are not reactivated. For example, in east Shetland Basin,
308 pre-existing faults that juxtapose sedimentary rocks against sedimentary rocks did not influence later rift geometry (Claringbould,
309 *et al.*, 2017). To our knowledge, the influence of a contrast in rheology between foot- and hanging wall rock on the likelihood of
310 fault reactivation is not well understood and forms an interesting topic for future research.

311 **Summary, conclusions and implications**

312 This case study documents the expression of a regional phase of rifting (Phase 2) on neighbouring terrains, both with and without a
313 set of pre-existing rift faults (Phase 1). The present study compares the findings of Henstra *et al*. (2015) from the North Træna Basin
314 to the neighbouring Ribban- and Vesfjorden basins. We demonstrate that Phase 2 faults evolved very differently in those areas
315 where a Phase 1 brittle imprint is absent. As such, the Lofoten Margin is a natural laboratory in which we can study the effect of
316 pre-existing structural heterogeneities on normal fault growth.

317 We conclude that:

318 - At the end of Permian–Triassic (Phase 1) rifting the Lofoten Margin consisted of a central area made up of exhumed
319 lower crustal rocks, juxtaposed to the east and to the west against areas consisting of upper crustal extensional basins. The
320 crystalline basement of the central area had a weak or absent brittle imprint whereas the neighbouring areas were
321 characterised by a pervasive set of NNE-SSW-striking normal faults inherited from Phase 1. After a *c.* 80 Myr-long inter-
322 rift period the Lofoten Margin became subjected to renewed rifting, starting in the Late Jurassic and peaking in the Early
323 Cretaceous (Phase 2).
324
325 - In the case of the Lofoten Margin, a factor that may have played an important role in the propensity of Phase 1 faults to
326 be reactivated during Phase 2 is a rotation of the regional extension direction that was invoked for the Lofoten Margin
327 (e.g. Henstra et al., 2015). A change to NW-SE-directed extension during the Phase 2 would have been favourable for the
328 linkage of the generally right-stepping, NNE-SSW-striking Phase 1 faults.
329

- The present case study demonstrates that the presence of older rift faults may exert a major control on fault growth during subsequent rift episodes by means of reactivation. Where older rift faults are present, these may be reactivated and control the localisation, segmentation, orientation and dimensions of later phase fault zones, resulting in faults with strong zigzag plan-view geometries, or faults that are strongly reoriented and oblique compared to the main stretching direction (see e.g. Henza et al. 2010, 2011, Rotevatn et al., 2018a). Conversely, where pre-existing structural grains are absent, the development of collinear through-going fault zones orientated orthogonal to the direction of extension may be expected (e.g. as seen herein; see also Henza et al. 2010, 2011)

- We hypothesize that a factor that may play a major role in the likelihood of reactivation of pre-existing faults in multiphase rifts is the contrast between foot- and hanging wall lithology/rheology. Where pre-existing faults juxtapose relatively weak siliciclastic rocks against a rigid crystalline footwall such as in Lofoten, the resultant strong heterogeneities are likely to be long-lived, independent of healing of the fault itself, and may therefore become subject to stress concentration and strain localisation during renewed rifting.

- Understanding the key controls of inheritance on rift development is crucial, and we have here demonstrated how the presence or absence of a pre-existing fault network may strongly influence the development of later faults. This is important since fault array development has implications for understanding basin physiography, sediment routing and dispersal, and the location and migration of depocentres during rift development. This in turn has economic implications, since these are factors that determine the location of sand fairways and, therefore, potential reservoirs for hydrocarbons exploitation or carbon storage in the subsurface.

**Acknowledgements**

We acknowledge Norske Shell for funding and data access. We especially wish to thank Rodmar Ravnås (formerly Norske Shell) for support. Schlumberger is thanked for licensing the Petrel software package to the University of Bergen. Permission to publish seismic data was kindly granted by PL219 partners. The geology department at the University of Otago is thanked for hosting A. Rotevatn on a research sabbatical, during which he contributed to this paper. Rebecca Bell, Ken McCaffrey, one anonymous reviewer and especially Johan Claringbould provided a range of insightful comments that helped us to improve the paper.

**References**

ACOCELLA, V., GUDMUNDSSON, A. & FUNICIELLO, R. (2000) Interaction and linkage of extension fractures and normal faults: examples from the rift zone of Iceland. *Journal of Structural Geology*, 22, 1233–1246.

ANDERSEN, T.B., JAMTVEIT, B., DEWEY, J.F. & SWENSON, E. (1991) Subduction and eduction of continental crust: Major mechanisms during continent-continent collision and orogenic extensional collapse, a model based on the southern Norwegian Caledonides. *Terra Nova*, 3, 303–310.

BELL, R.E., JACKSON, C.A-L., WHIPP, P.S. & CLEMENTS, B. (2014) Strain migration during multiphase extension: Observations from the northern North Sea. *Tectonics*, 33, 1936–1963.

BELLAHSEN, N., FOURNIER, M., D'ACREMONT, E., LEROY, S. & DANIEL, J.M. (2006) Fault reactivation and rift localization: Northeastern Gulf of Aden margin. *Tectonics*, 25, 1–14.

BERGH, S.G., EIG, K., KLØVJAN, O.S., HENNINGSEN, T., OLESEN, O. & HANSEN, J.-A. (2007) The Lofoten-Vesterålen continental margin: a multiphase Mesozoic-Palaeogene rifted shelf as shown by offshore-onshore brittle fault-fracture analysis. *Norwegian Journal of Geology*, 87, 29–58.

BRUNE, S., POPOV, A.A. & SOBOLEV, S.V. (2012) Modeling suggests that oblique extension facilitates rifting and continental break-up. *Journal of Geophysical Research: Solid Earth*, 117, 1–16.

CHILDS, C., WATTERSON, J. & WALSH, J.J. (1995) Fault overlap zones within developing normal fault systems. *Journal of the Geological Society*, 152, 535–549.

CLARINGBOULD, J.S., BELL, R.E., JACKSON, C.A.L., GAWTHORPE, R.L. & ODINSEN, T. (2017) Pre-existing normal faults have limited control on the rift geometry of the northern North Sea. *Earth and Planetary Science Letters*, 475, 190–206.

COWIE, P.A. (1998) Normal fault growth in three-dimensions in continental and oceanic crust. *In: Faulting and Magmatism at Mid-Ocean Ridges (Ed. by R. Buck, P. Delaney, J. Karson and Y. Lagabrielle)*, AGU Monograph 106.

COWIE, P.A., GUPTA, S. & DAWERS, N.H. (2000) Implications of fault array evolution for synrift depocentre development: insights from a numerical fault growth model. *Basin Research*, 12, 241–261.

CRIDER, J.G. & POLLARD, D.D., (1998) Fault linkage: Three-dimensional mechanical interaction between echelon normal faults. *Journal of Geophysical Research: Solid Earth*, 103, 24373–24391.

DAVIES, R.J., TURNER, J.D. & UNDERHILL, J.R. (2001) Sequential dip-slip movement during rifting: A newmodel for the evolution of the Jurassic trilete North Sea rift system. *Petroleum Geoscience*, 7, 371–388.

DENG, C., GAWTHORPE, R.L., FINCH, E. & FOSSEN, H. (2017) Influence of a pre-existing basement weakness on normal fault growth during oblique extension: Insights from discrete element modeling. *Journal of Structural Geology*.

DORÉ, A.G. (1992) Synoptic palaeogeography of the Northeast Atlantic Seaway: late Permian to Cretaceous. *In: Parnell, J. (Ed.), Basins on the Atlantic Seaboard: Petroleum Geology, Sedimentology and Basin Evolution*. Geological Society, London, Special Publications, 62, 421–446.

DORÉ, A.G., LUNDIN, E.R., JENSEN, L.N., BIRKELAND, Ø., ELIASSEN, P.E. & FICHLER, C. (1999) Principal tectonic events in the evolution of the northwest European Atlantic margin. *In: Fleet, A.J., Boldy, S.A. (Eds.), Petroleum Geology of Northwest Europe.* Proceedings of the 5th Conference, 41–62.

EHRLICH, R. & GABRIELSEN, R.H. (2004) The complexity of a ramp–flat–ramp fault and its effect on hanging-wall structuring: an example from the Njord oil field, offshore mid-Norway. *Petroleum Geoscience*, 10, 305–317.

ETHERIDGE, M.A. (1986) On the reactivation of extensional fault systems. *Phil. Trans. R. Soc. Lond. A*, 317, 179–194.

FALEIDE, J.I., BJØRLYKKE, K & GABRIELSEN, R.H. (2010) Geology of the Norwegian Continental Shelf. *In: Bjørlykke, K.: Petroleum Geoscience: From Sedimentary Environments to Rock Physics*. Springer-Verlag, Berlin Heidelberg, 467–499.

FÆRSETH, R.B. (2012) Structural development of the continental shelf offshore Lofoten–Vesterålen, northern Norway. *Norwegian Journal of Geology*, 92, 19–40.

GIBA, M., WALSH, J. & NICOL, A. (2012) Segmentation and growth of an obliquely reactivated normal fault. *Journal of Structural Geology*, 39, 253–267.

GUPTA, S., COWIE, P.A., DAWERS, N.H. & UDERHILL, J.R. (1998) A mechanism to explain rift-basin subsidence and stratigraphic patterns through fault array evolution. *Geology*, 26, 595–598.

HAMES, W.E. & ANDRESEN, A. (1996) Timing of Palaeozoic orogeny and extension in the continental shelf of north-central Norway as indicated by laser 40Ar/ 39Ar muscovite dating. *Geology*, 24, 1005–1008.

HANSEN, J.W, BAKKE, S. & FANAVOLL, S. (1992) Shallow drilling Nordland VI and VII 1992. IKU report 23.

HANSEN, J.-A., BERGH, S.G. & HENNINGSEN, T. (2012) Mesozoic rifting and basin evolution on the Lofoten and Vesterålen Margin, North-Norway; time constraints and regional implications. *Norwegian Journal of Geology,* 91, 203–228.

HENSTRA, G.A. & ROTEVATN, A. (2014) Nature of Palaeozoic extension in Lofoten, north Norwegian Continental Shelf: insights from 3-D seismic analysis of a Cordilleran-style metamorphic core complex. *Terra Nova*, 26, 247–252.

HENSTRA, G.A., ROTEVATN, A., GAWTHORPE, R.L. & RAVNÅS, R. (2015) Evolution of a major segmented normal fault during multiphase rifting: the origin of plan-view zigzag geometry. *Journal of Structural Geology*, 74, 45–63.

HENSTRA, G.A., GAWTHORPE, R.L., HELLAND-HANSEN, W., RAVNÅS, R. & ROTEVATN, A. (2017) Depositional systems in multiphase rifts: seismic case study from the Lofoten margin, Norway. *Basin Research*, 29, 447–469.

HENZA, A.A., WITHJACK, M.O. & SCHLISCHE, R.W. (2010) Normal-fault development during two phases of non-coaxial extension: An experimental study. *Journal of Structural Geology*, 32, 1656–1667.

HENZA, A.A., WITHJACK, M.O. & SCHLISCHE, R.W. (2011) How do the properties of a pre-existing normal-fault population influence fault development during a subsequent phase of extension? *Journal of Structural Geology*, 33, 1312–1324.

HUYGHE, P. & MUGNIER, J.L. (1992) The influence of depth on reactivation in normal faulting. *Journal of Structural Geology*, 14, 991–998.

JACKSON, C.A.L. & ROTEVATN, A. (2013) 3D seismic analysis of the structure and evolution of a salt-influenced normal fault zone: a test of competing fault growth models. *Journal of Structural Geology*, 54, 215–234.

KEEP, M. & MCCLAY, K.R. (1997) Analogue modeling of multiphase rift systems. *Tectonophysics*, 273, 239–270.

KLEIN, A.C., STELTENPOHL, M.G., HAMES, W.E. & ANDRESEN, A. (1999) Ductile and brittle extension in the southern Lofoten Archipelago, North Norway; implications for differences in tectonic style along an ancient collisional margin. *American Journal of Science*, 299, 69–89.

LAUBACH, S.E., EICHHUBL, P., HARGROVE, P., ELLIS, M.A. & HOOKER, J.N. (2014) Fault core and damage zone fracture attributes vary along strike owing to interaction of fracture growth, quartz accumulation, and differing sandstone composition. *Journal of Structural Geology*, 68, 207–226.

LEE, M.J.& HWANG, Y.J. (1993) Tectonic evolution and structural styles of the East Shetland Basin. *Geological Society, London, Petroleum Geology Conference series*, 4, 1137–1149.

LEPVRIER, C., FOURNIER, M. BERARD, T. & ROGER, J. (2002). Cenozoic extension in coastal Dhofar (southern Oman): implications on the oblique rifting on the Gulf of Aden. *Tectonophysics*, 357, 279–293.

LØSETH, H. & TVETEN, E. (1996) Post-Caledonian structural evolution of the Lofoten and Vesterålen offshore and onshore areas. *Norwegian Journal of Geology*, 76, 215–230.

MACGREGOR, D. (2015) History of the development of the East African Rift System: a series of interpreted maps through time. *Journal of African Earth Sciences*, 101, 232–252.

MATS, V.D. & PEREPELOVA, T.I. (2011) A new perspective on evolution of the Baikal Rift. *Geoscience Frontiers*, 2, 349–365.

MCLEOD, A., DAWERS, N.H. & UNDERHILL, J.R. (2000) The propagation and linkage of normal faults: insights from the Strathspey–Brent–Statfjord fault array, northern North Sea. *Basin Research*, 12, 263–284.

MJELDE, R. & SELLEVOLL, M.A. (1993) Possible shallow crustal shear wave anisotropy off Lofoten, Norway, inferred from three-component ocean-bottom seismographs. *Geophysical Journal International*, 115, 159–167.

MORLEY, C.K., HARANYA, C., PHOOSONGSEE, W., PONGWAPEE, S., KORNSAWAN, A. & WONGANAN, N. (2004) Activation of rift oblique and rift parallel pre-existing fabrics during extension and their effect on deformation style: examples from the rifts of Thailand. *Journal of Structural Geology*, 26, 1803–1829.

MOSAR, J., EIDE, E.A., OSMUNDSEN, P.T., SOMMARUGA, A. & TORSVIK, T.H. (2002) Greenland – Norway separation: A geodynamic model for the North Atlantic. *Norwegian Journal of Geology*, 82, 281–298.

NIXON, C.W., McNEILL, L. C., BULL, J.M., BELL, R.E., GAWTHORPE, R.L. & HENSTOCK, T.J. (2016) Rapid spatiotemporal variations in rift structure during development of the Corinth Rift, Central Greece. *Tectonics*, 35, 1225–1248

NØTTVEDT, A., JOHANNESSEN, E.P. & SURLYK, F. (2008) The mesozoic of western Scandinavia and East Greenland. *Episodes*, 31, 59–65.

PEACOCK, D.C.P. & SANDERSON, D. J. (1991). Displacements, segment linkage and relay ramps in normal fault zones. *Journal of Structural Geology*, 13, 721–733.

PERON-PINVIDIC, G., MANATSCHAL, G. & OSMUNDSEN, P.T. (2013). Structural comparison of archetypal Atlantic rifted margins: A review of observations and concepts. *Marine and Petroleum Geology*, 43, 21–47.

PHILLIPS, T.B., JACKSON, C.A.L., BELL, R.E., DUFFY, O.B. & FOSSEN, H. (2016) Reactivation of intrabasement structures during rifting: A case study from offshore southern Norway. *Journal of Structural Geology*, 91, 54–73.

PROSSER, S. (1993) Rift-related linked depositional systems and their seismic expression. *In: Williams, G.D., Dobb, A. (Eds.), Tectonics and seismic sequence stratigraphy*. The Geological Society of London, London, 35–66.

RAVNÅS, R., NØTTVEDT, A., STEEL, R.J. & WINDELSTAD, J. ( 2000) Syn-rift sedimentary architectures in the Northern North Sea. *In: Nøttvedt, A. (Ed.), Dynamics of the Norwegian Margin.* Geological Society, London, Special Publications, 167, 133–177.

ROTEVATN, A. & JACKSON, C.A.L. (2014) 3D structure and evolution of folds during normal fault dip linkage. *Journal of the Geological Society*, 171, 821–829.

ROTEVATN, A., KRISTENSEN, T.B., KSIENZYK., A.K., WEMMER, K., HENSTRA, G.A., MIDTKANDAL, I., GRUNDVÅG, S.-A. & ANDRESEN, A. (2018a) Structural Inheritance and Rapid Rift-Length Establishment in a Multiphase Rift: The East Greenland Rift System and its Caledonian Orogenic Ancestry. *Tectonics*, 37, 1858–1875

ROTEVATN, A., JACKSON, C.A.L., TVEDT, A.B.M., BELL, R. & BLÆKKAN, I. (2018b) How Do Normal Faults Grow? Journal of Structural Geology. doi:10.1016/j.jsg.2018.08.005

STELTENPOHL, M.G., HAMES, W.E. & ANDRESEN, A. (2004) The Silurian to Permian history of a metamorphic core complex in Lofoten, northern Scandinavian Caledonides. *Tectonics*, 23, 1–23.

STELTENPOHL, M.G., KASSOS, G. & ANDRESEN, A. (2006) Retrograded eclogite facies pseudotachylytes as deep-crustal paleoseismic faults within continental basement of Lofoten, north Norway: *Geosphere*, 2, 61–72. doi:10.1130/GES00035.1.

TENTHOREY, E. & COX, S.F. (2006) Cohesive strengthening of fault zones during the interseismic period: An experimental study. *Journal of Geophysical Research: Solid Earth*, 111. doi:10.1029/2005JB004122
F2006

TOMASSO, M., UNDERHILL, J.R., HODGKINSON, R. A. & YOUNG, M.J. (2008) Structural styles and depositional architecture in the Triassic of the Ninian and Alwyn North fields: Implications for basin development and prospectivity in the Northern North Sea. *Marine and Petroleum Geology*, 25(7), 588-605.

TSIKALAS, F., FALEIDE, J.I. & ELDHOLM, O. (2001) Lateral variations in tectono-magmatic style along the Lofoten-Vesterålen volcanic margin off Norway. *Marine and Petroleum Geology*, 18, 807–832.

WALSH, J.J., NICOL, A. & CHILDS, C. (2002) An alternative model for the growth of faults. *Journal of Structural Geology*, 24, 1669–1675.

WHIPP, P.S., JACKSON, C.A-L., GAWTHORPE, R.L., DREYER, T. & QUINN, D. (2014) Normal fault array evolution above a reactivated rift fabric; a subsurface example from the northern Horda Platform, Norwegian North Sea. *Basin Research*, 26, 523–549. doi: 10.1111/bre.12050

WILSON, R.W., MCCAFFREY, K.J.W., HOLDSWORTH, R.E., IMBER, J., JONES, R.R., WELBON, A.I.F. & ROBERTS, D. (2006) Complex fault patterns, transtension and structural segmentation of the Lofoten Ridge, Norwegian margin; using digital mapping to link onshore and offshore geology. *Tectonics*, 25, 1–28.

**Figure Captions**

**Fig. 1**. (**a**) Location of the Lofoten Margin located offshore northern Norway. (**b**) The Base Cretaceous two-way travel time (TWTT) structure map illustrates the structural framework of the Lofoten Margin within the area of interest. Line c-c' marks the locations of the cross section shown in c. The depth to Moho is indicated in km-scale yellow contour lines. (c) Cross section through the main structural elements of the Lofoten Margin: from west to east the Røst High, the North Træna Basin, the Marmæle Spur, the Ribban Basin, the Lofoten Ridge and the Vestfjorden Basin.

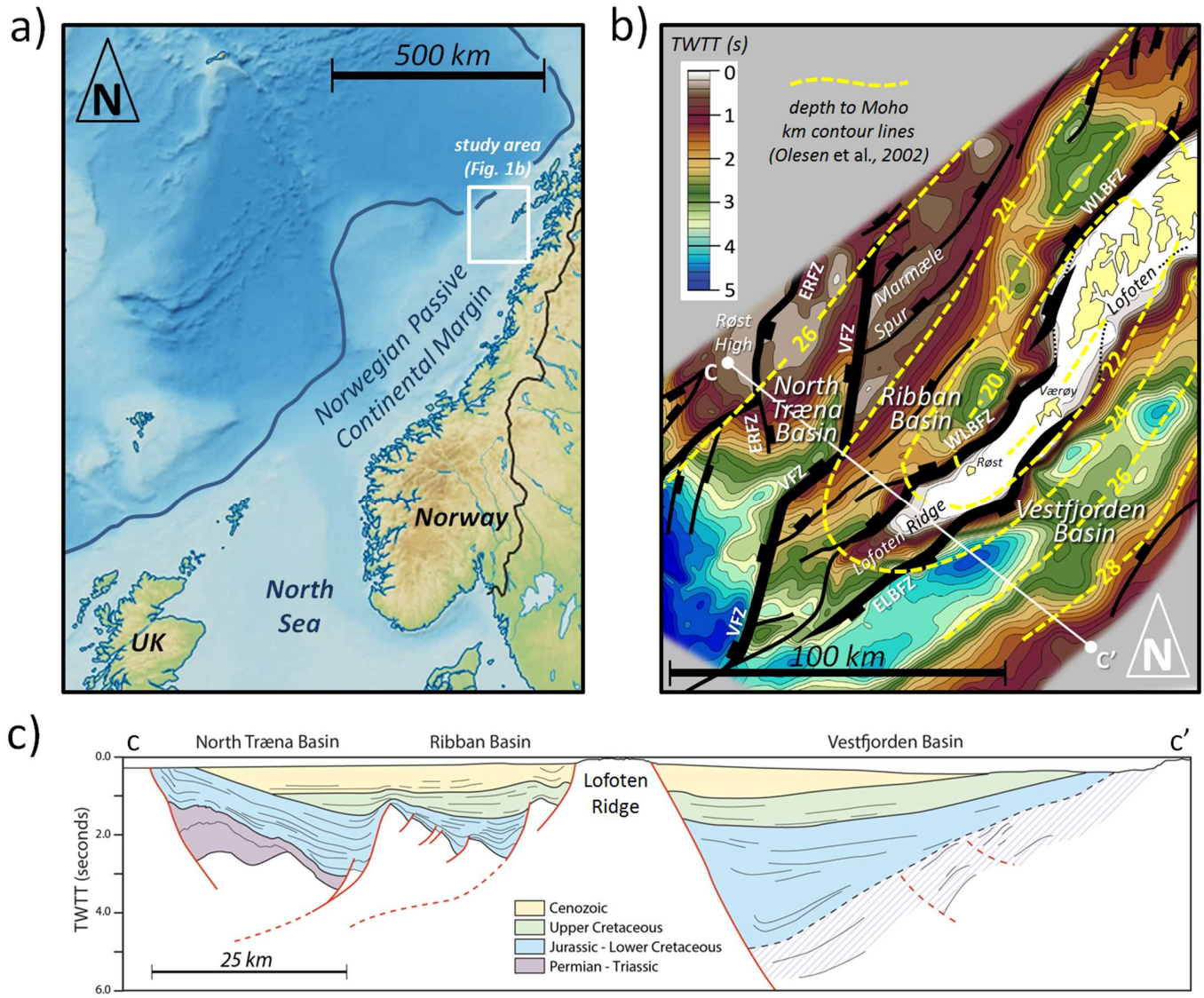

**Fig. 2.** Interpreted representative seismic section of the North Træna Basin and the Ribban Basin. Location of the section (line 1) is indicated in Fig. 4.

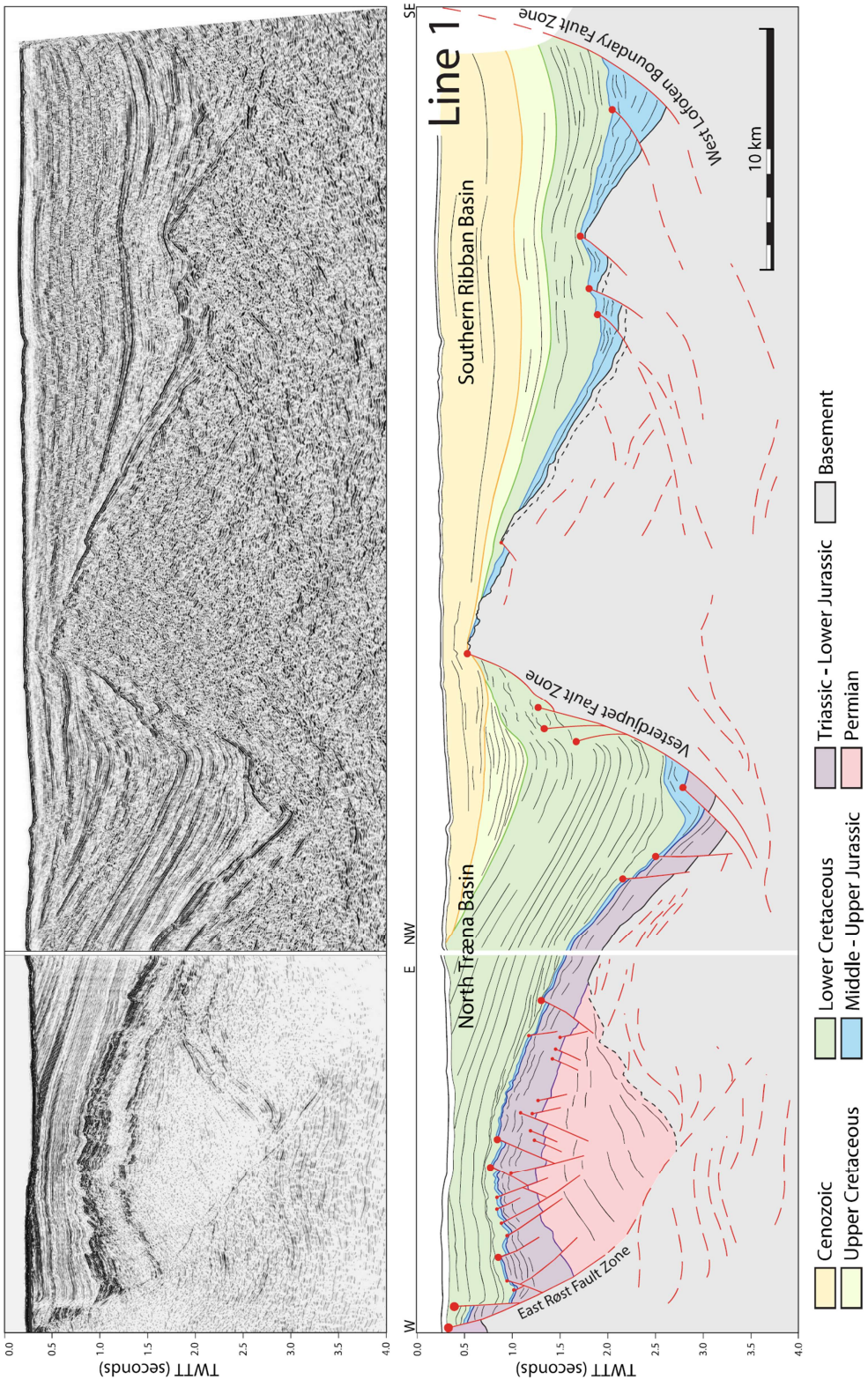

560 **Fig. 3.** Available seismic and well data in the area of interest. In this study new results from mapping of the Ribban Basin (sector
561 2) are presented. Data availability for sectors 1 and 3 are included here to show datasets used in previous studies.

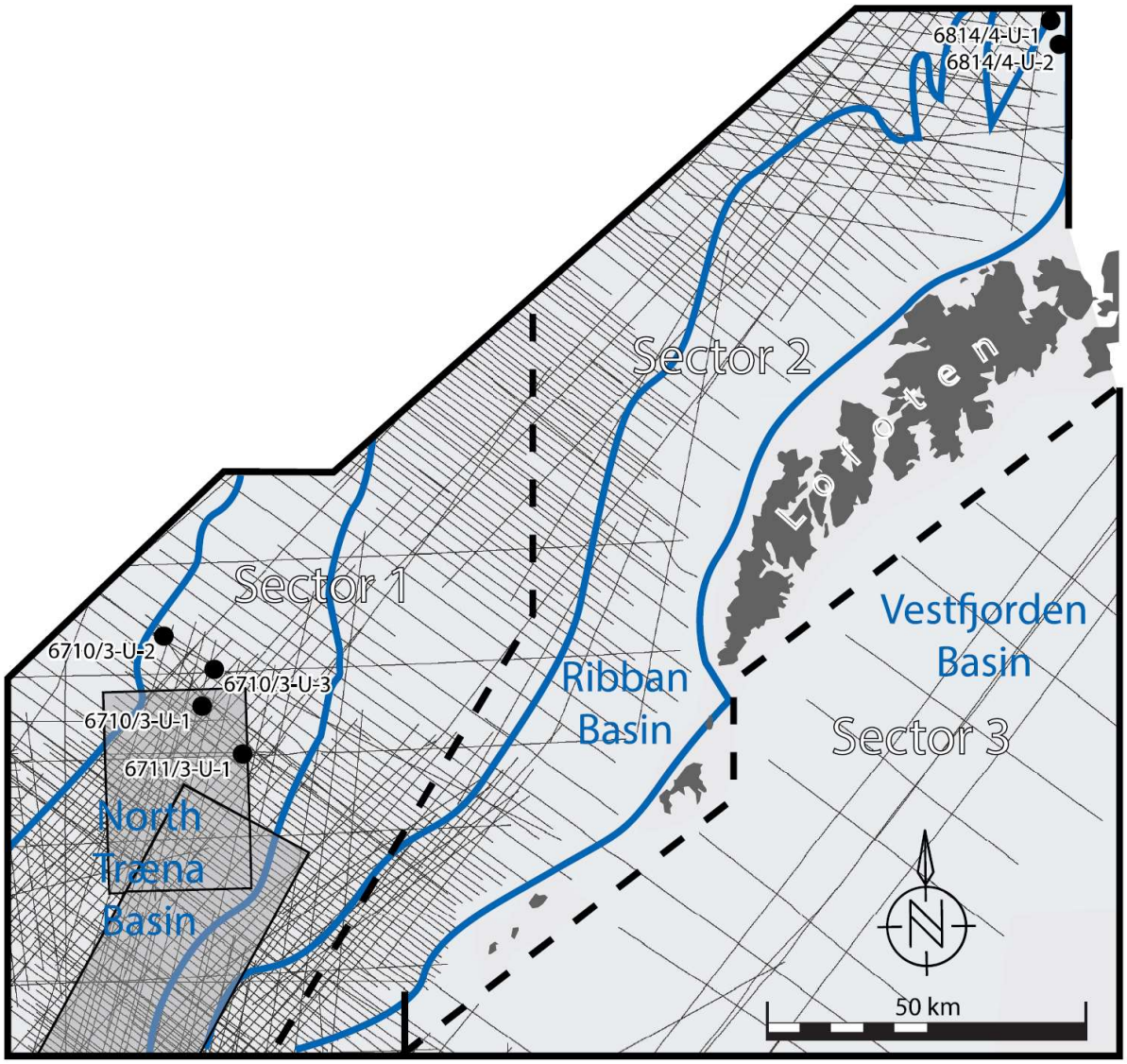

562 **Fig. 4.** Base Cretaceous structure map in two-way travel time. The map shows the structure across the North Træna Basin (sector
563 1, Fig. 3) as previously presented by Henstra *et al*. (2015) as well as new results for the Ribban Basin (sector 2, Fig. 3) presented
564 in this paper. Dashed lines indicate the approximate extent of Upper Jurassic depocentres (blue) and the area where the Upper
565 Cretaceous and younger strata are entirely removed (green).

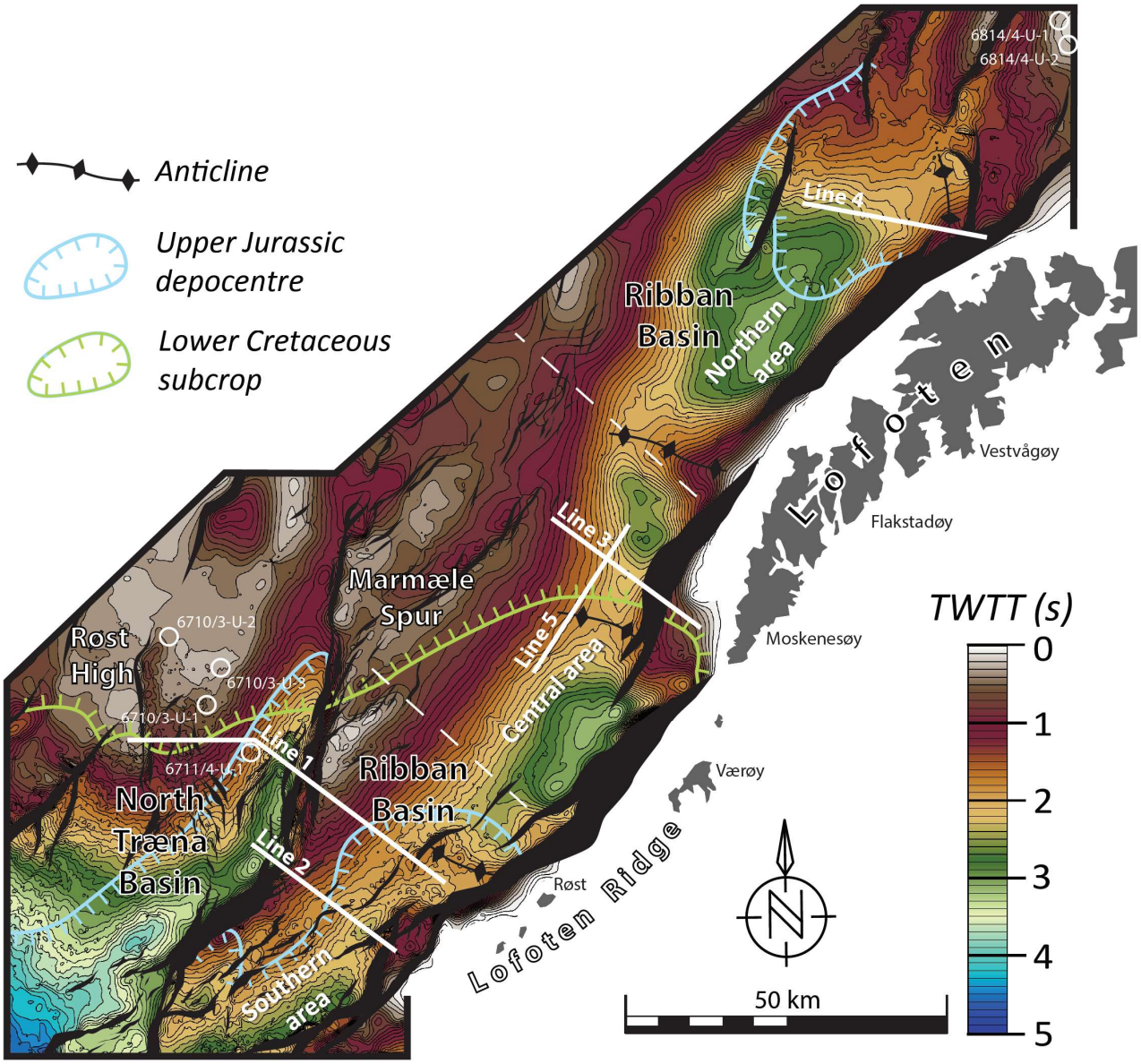

**Fig. 5.** Interpreted representative seismic sections for the northern-, central- and southern areas of the Ribban Basin. Locations are indicated in Fig. 4. Striped red lines indicate intra-basement reflections.

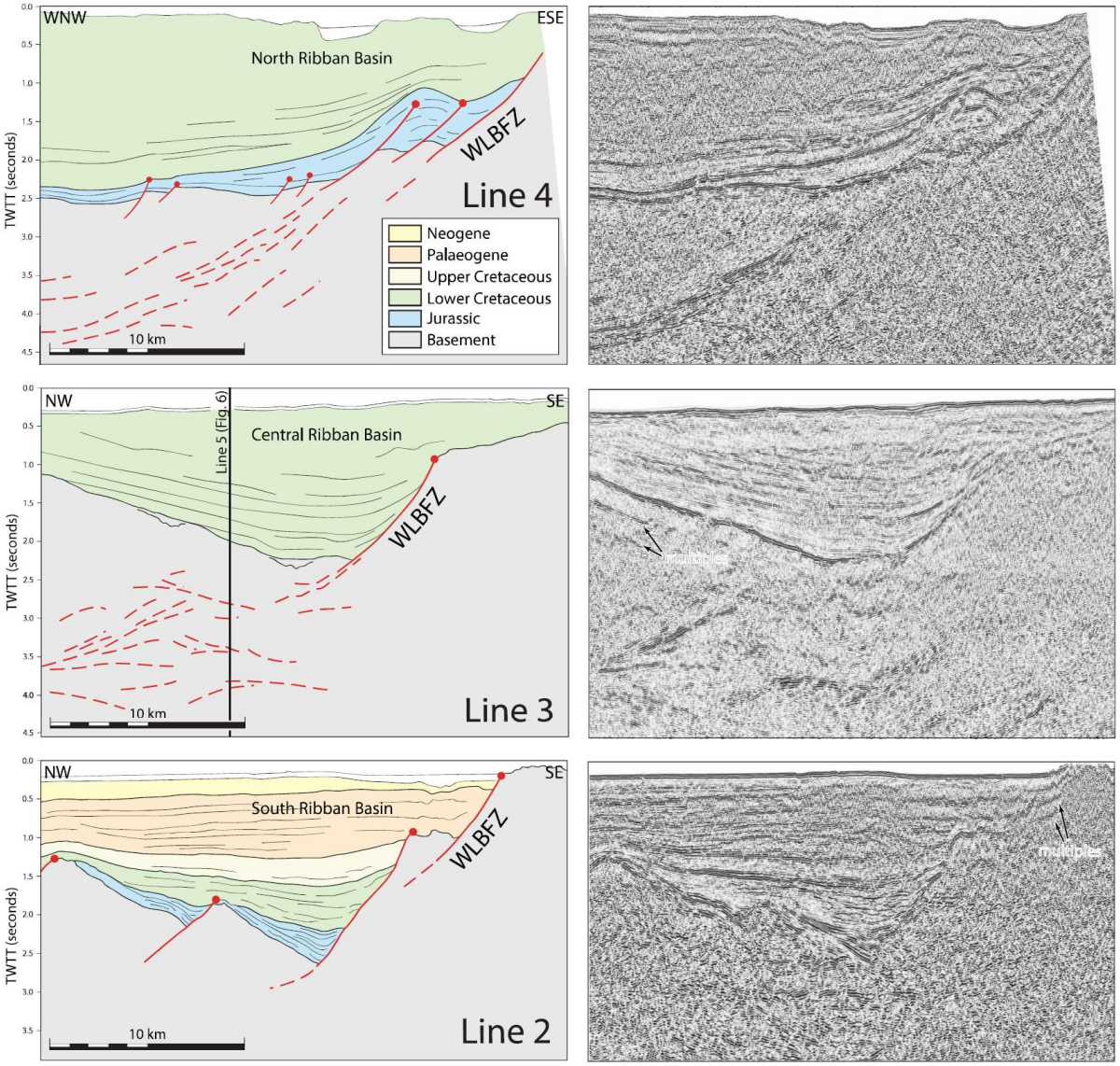

568 **Fig. 6.** Interpreted seismic strike-section for the central area. Lines 3 and 5 cross one another as indicated on both sections.
569 Location is indicated in Fig. 4.

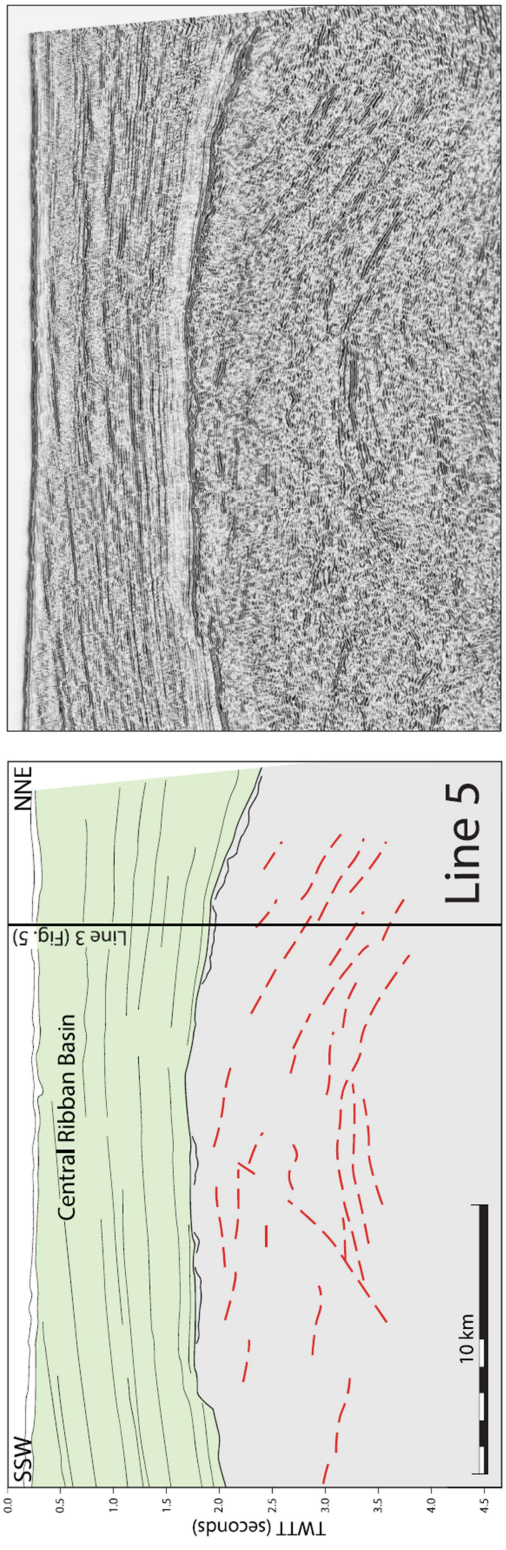

**Fig. 7.** The distribution of normal faults and associated depocentres on the Lofoten Margin through time: (**a**) Permian; (**b**) Triassic; (**c**) Jurassic and (**d**) Cretaceous. The hatched area in Fig. 7a indicates the approximate outline of the metamorphic core of the MCC.

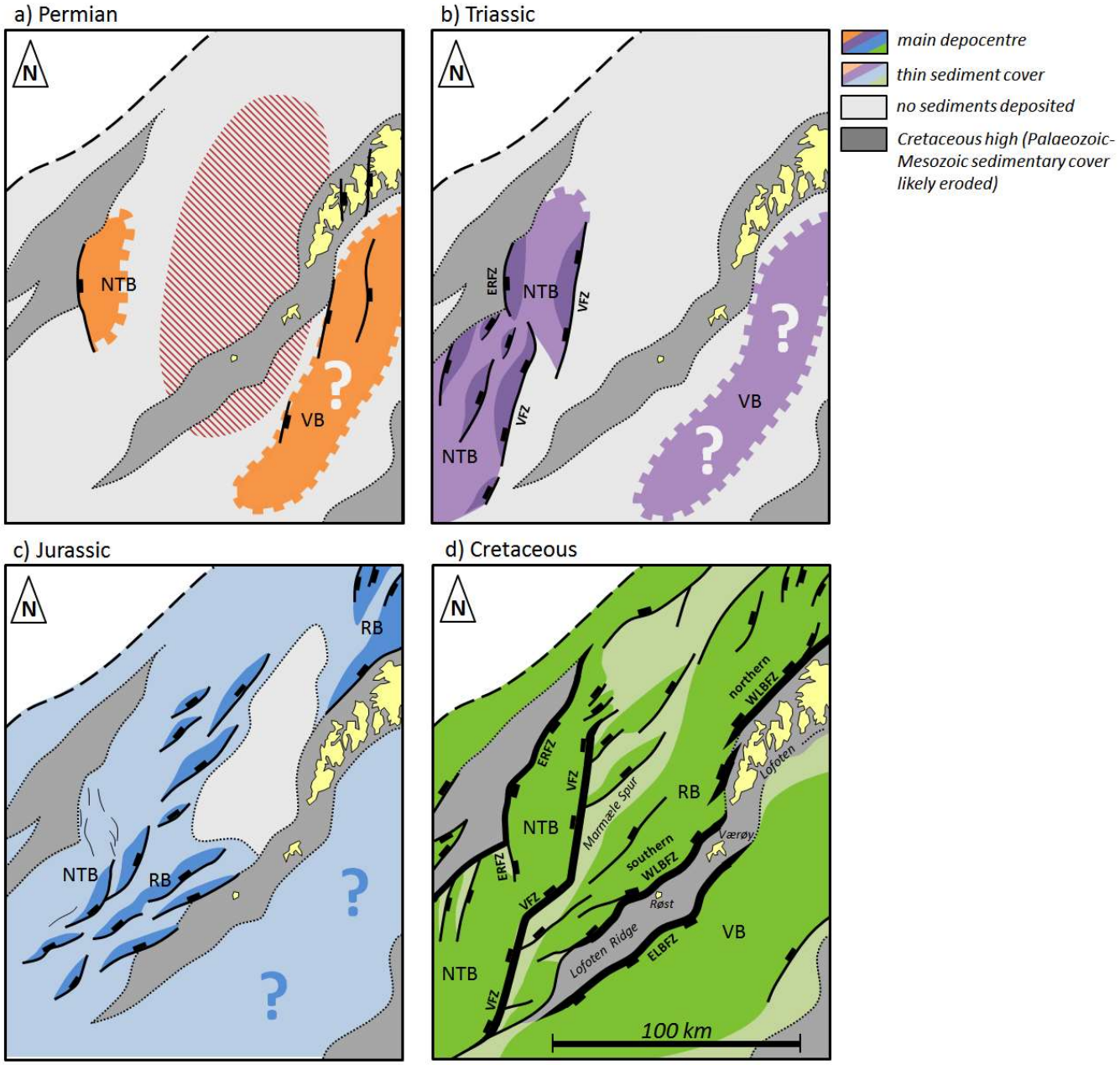

**Fig. 8.** Schematic 3-D block diagram illustrating the distribution and geometry of faults and basins for the different studied rift phases of the Lofoten Margin, as well as the nature of basin-fill from Permian to Cretaceous times. Note that the ERFZ and the VFZ initiated in Phase 1, whereas the ELBFZ and WLBFZ only became active in Phase 2.

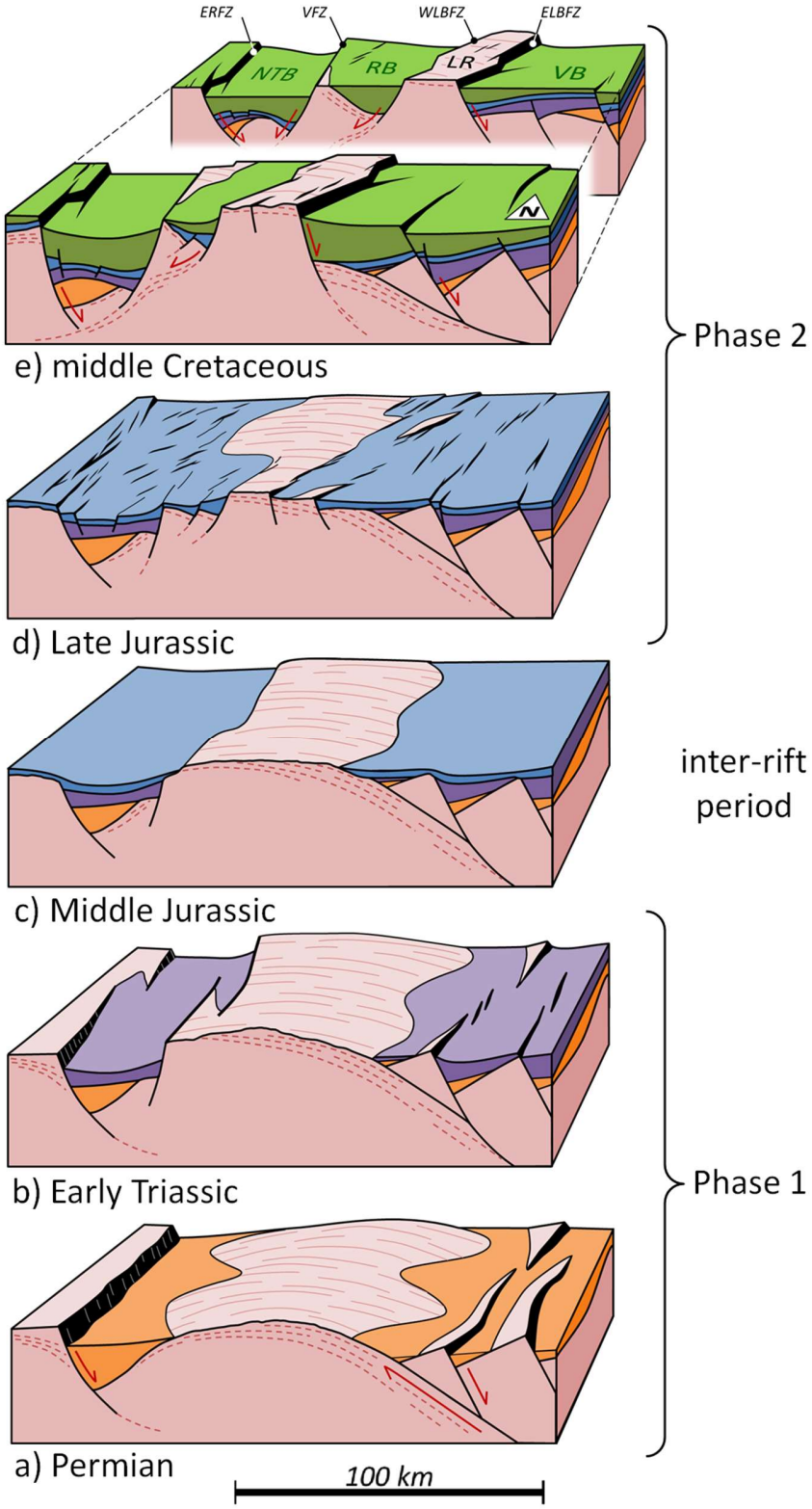

**Fig. 9.** Interpreted structural framework of the Lofoten Margin. The ERFZ and VFZ that bound the North Træna Basin consist of reactivated Phase 1 segments (red) as well as segments that first formed in Phase 2 (blue). The WLBFZ and ELBFZ consist exclusively of Phase 2 segments. The hatched area provides a very rough outline of the geographic extent of the central zone of the Permian core complex, where the crystalline basement lacks a Phase 1 brittle imprint. The outline is based on the presence of basement reflections that are sub-parallel to the basement-sediment interface and the onlapping relationship between basement and Jurassic and Lower Cretaceous strata.

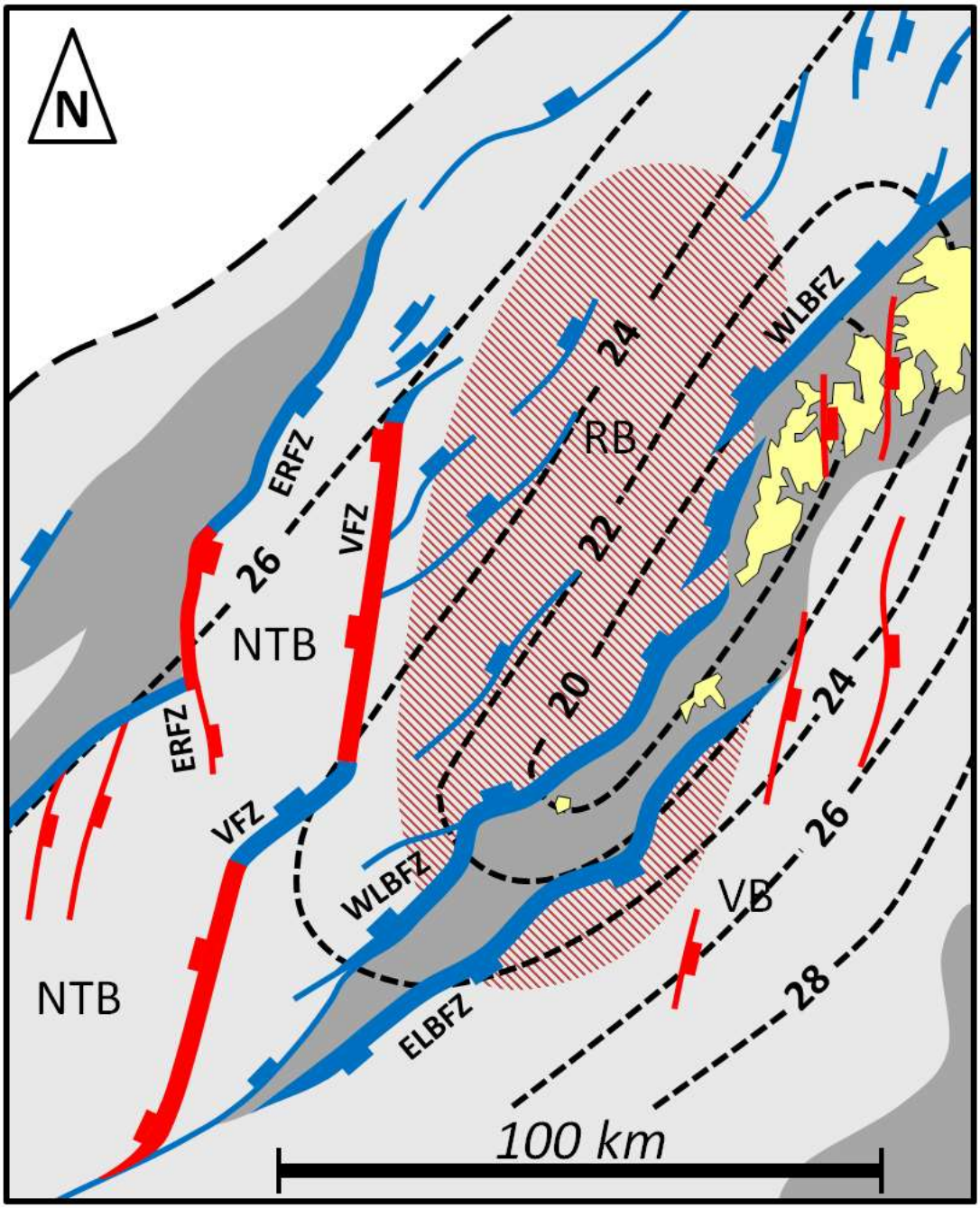

**Fig. 10.** Contrasting styles of fault growth as a consequence of the presence (**a–d**) or absence (**e–h**) of pre-existing structural heterogeneities. Characteristic features of Phase 2 faults that grow by reactivation of Phase 1 faults are i) the development of through-going fault zones that strike at an angle to the prevailing direction of extension; ii) the development of zigzag geometries rather than collinear fault zones and iii) the development of splay faults that strike orthogonal to the direction of Phase 2 extension, typically at the tips of reactivated Phase 1 faults. These models are based on findings from the present study as well as the results of Henza *et al*. (2011) and Whipp *et al*. (2014).